Material Science Research India Vol. **12**(1), 08-14 (2015)

Magnetic properties of $SrFe_{12-x}Al_xO_{19}$

I. BSOUL* and W. I. DA'AS

Physics Department, Al al-Bayt University, Mafraq 130040, Jordan.

http://dx.doi.org/10.13005/msri/120102

(Received: May 02, 2015; Accepted: May 14, 2015)

ABSTRACT

In this work, pure and doped with Al (Aluminum) strontium hexaferrite ($SrFe_{12-x}Al_xO_{19}$) were fabricated by solid state reaction method. The Al concentration (x) for the fabricated samples was varied from x=0.0 to x=0.6. Structural and magnetic properties of the fabricated samples were investigated. Analyses of XRD data showed that all samples of high quality, since the measured XRD patterns found to match the standard pattern for single phase of $SrFe_{12}O_{19}$. The lattice constants a and c were calculated. It was found that the replacement of Fe^{3+} with Al^{3+} ions in hexagonal strontium ferrite led to a negligible changes in lattice constant a, whereas the hexagonal lattice constant c found to decrease with increasing the substitution amount of Al. The crystallite size was also determined using the XRD data. It has been found that that Al^{3+} substitution for Fe^{3+} does not appreciably disturb the crystallinity of $SrFe_{12-x}Al_xO_{19}$, since the crystallite size for all samples ranged from 83 – 72 nm. The magnetic data showed that doping of strontium with Al leads to a small decrease in saturation magnetization. Also it has been found that the doping of strontium ferrite with Al leads to an increase in the coercivity as a result of increasing of the anisotropy field.

Key words: Solid state reaction, Strontium ferrite, Coercive field, Anisotropy field.

INTRODUCTION

Strontium ferrite compound ($SrFe_{12}O_{19}$) belongs to hexaferrite group, which attracts a considerable attention due to their enormous ability to be used as storage media and the fabrication of permanent magnets. Fabrication method plays an important role in determining the magnetic, electrical and some structural properties of the end product. Also the magnetic properties can be controlled by the replacement of magnetic Fe^{3+} ions by a wide range of magnetic and nonmagnetic cations such as Co, Ni, Zn, Ga, Al, Cr,Ti[1-5] or cations combination such as Mg-Zr, Co-Nd Ni-Sn, Ni-Ru, Zn-Ru, Co-Ti, Ti-Ru[6-15]. These substitutions aim for the development of improved hexaferrite compounds that can be utilized in technological purposes.

Experimental procedures

$SrFe_{12-x}Al_xO_{19}$ powders with x = 0, 0.1, 0.2, 0.3, 0.4, 0.5 and 0.6 were prepared by solid state method. Metallic oxides (Fe_2O_3, and Al_2O_3) and strontium carbonate ($SrCO_3$) were used to fabricate pure and doped with aluminum strontium ferrite powders. Metallic oxides were weight in appropriate amount then loaded into a hardened stainless steel bowels with ball to powder ratio of 8:1. The milling process was carried out at 250 rpm for 16h. The resulting precursor was annealed at 1100°C for 2 h. XRD data was collected using Philips X'Pert PRO X-ray diffractometer (PW3040/60). The magnetic data were measured at room temperature using Princeton Measurements Corporation vibrating sample magnetometer (VSM). Rietveld refinement was used to refine XDR data using a will known FULLPROF suite package.

RESULTS AND DISCUSSION

Figure 1 shows the XRD patterns for all samples examined in this work (x = 0.0 to x = 0.6). All XRD patterns were identified by ICDD file (00-033-1340) which belongs to hexagonal strontium ferrite ($SrFe_{12}O_{19}$)[16]. Since only one phase is present

in all samples, we may conclude that the prepared samples are of high quality and the Al^{3+} ions diffused completely into the lattice of $SrFe_{12}O_{19}$. Rietveld refinement for all fabricated samples is also shown at Figure 1. Bragg factor (R_B) and the goodness of fit quality (χ^2) are shown in Table 1. The value of c^2 for all fitted samples nearly one, which indicates an excellent fit. The structural parameters for all samples are also tabulated in Table 1. The obtained lattice parameters agree well with the previously reported values for hexagonal strontium ferrite[17]. In this work, low doping level (x = 0.1 to x = 0.6) was investigated. XRD data showed that Al^{3+} substitution for Fe^{3+} in such low doping level does not affect the hexagonal structure of $SrFe_{12}O_{19}$. A negligible changes in lattice constant a can be seen in Table 1, whereas the hexagonal lattice constant c decrease with increasing the substitution amount of Al. The decrease of c can be referred to the difference in ionic radius, since the radius of Fe^{3+} ion, 0.645 Å, is larger than that for Al^{3+} ion, 0.51 Å. Hence the crystal structure becomes more compact and the unit cell

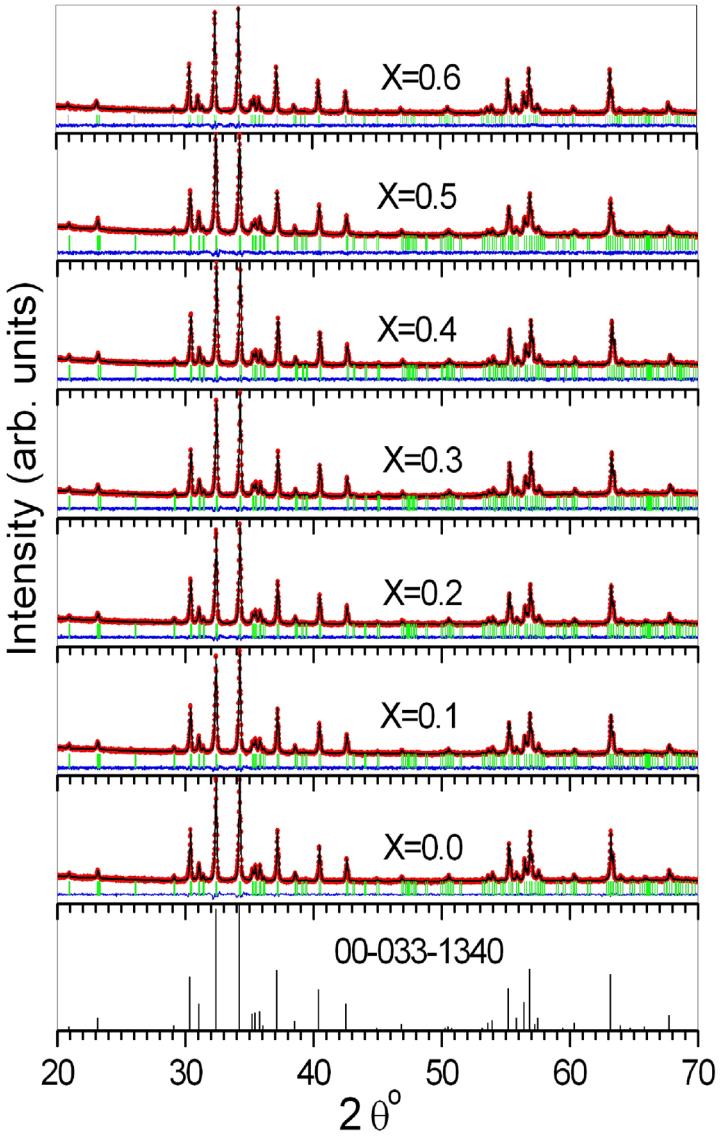

Fig. 1: Refined XRD patterns for $SrFe_{12-x}Al_xO_{19}$ samples along with standard ICDD pattern for $SrFe_{12}O_{19}$.

volume decreases as a result of Al^{3+} substitution. The crystallite size for the prepared samples was calculated according to Scherrer equation[18]:

$$D = \frac{K\lambda}{\beta \cos\theta} \quad ...(1)$$

where D is the crystallite size, K Scherrer constant, λ X-ray wavelength (1.54056 Å), β full width of half maximum, and θ is the peak position in degree. The (114) reflection was selected for the analysis, (after eliminating $K_{\alpha 2}$ components for more accuracy) since it is the strongest reflection. The results are tabulated in Table 1. From these data we may assume that Al^{3+} substitution for Fe^{3+} does not appreciably disturb the crystallinity of $SrFe_{12-x}Al_xO_{19}$, since the crystallite size for all samples ranged from 83 – 72 nm.

Figure 2 shows hysteresis loops for pure and doped strontium ferrite samples. The effect of Al^{3+} doping is clearly seen on the coercivity and saturation magnetization. As it was reported the magnetic moment in hexaferrites comes from Fe ions at different interstitial sites and can be given according to the equation[19-21]:

$$\vec{m} = \overrightarrow{2a} + \overrightarrow{2b} + \overrightarrow{12k} + \overrightarrow{4f_1} + \overrightarrow{4f_2} \quad ...(2)$$

The spin-down sites ($4f_1$ and $4f_2$) have two Fe ions each, whereas the spin-up sites 2*a* and 2*b*

Table 1: Bragg factor, χ^2, lattice constants *a* and *c*, unit cell volume and crystallite size of $SrFe_{12-x}Al_xO_{19}$

x	R_B	χ^2	a = b (Å)	c (Å)	V $(Å)^3$	D (nm)
0.0	2.69	1.103	5.8814	23.0355	690.0658	83
0.1	2.08	1.066	5.8798	23.0291	689.4998	82
0.2	2.47	1.072	5.8783	23.0234	688.9736	82
0.3	2.33	0.9735	5.8786	23.0302	689.2589	72
0.4	1.80	0.9497	5.8767	23.0227	688.5897	74
0.5	1.76	0.8768	5.8738	23.0069	687.4166	77
0.6	1.62	0.8493	5.8728	23.0031	687.0798	74

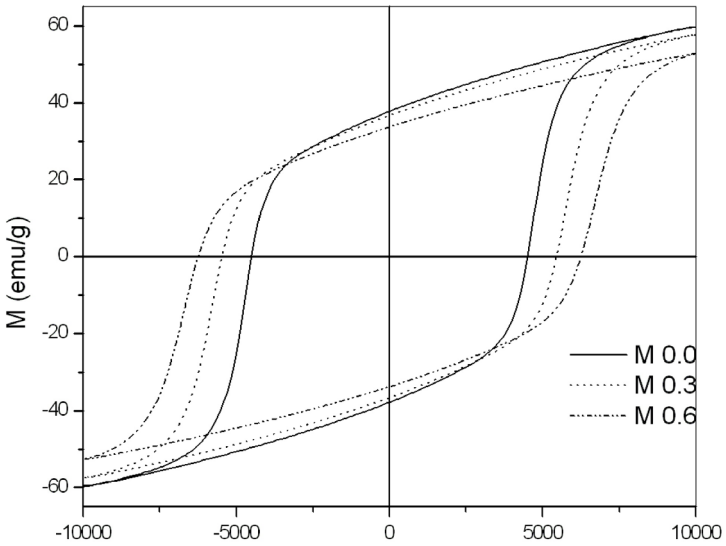

Fig. 2: Hysteresis loops for pure strontium ferrite and strontium ferrite doped with Al (x = 0.3 and x=0.6) samples.

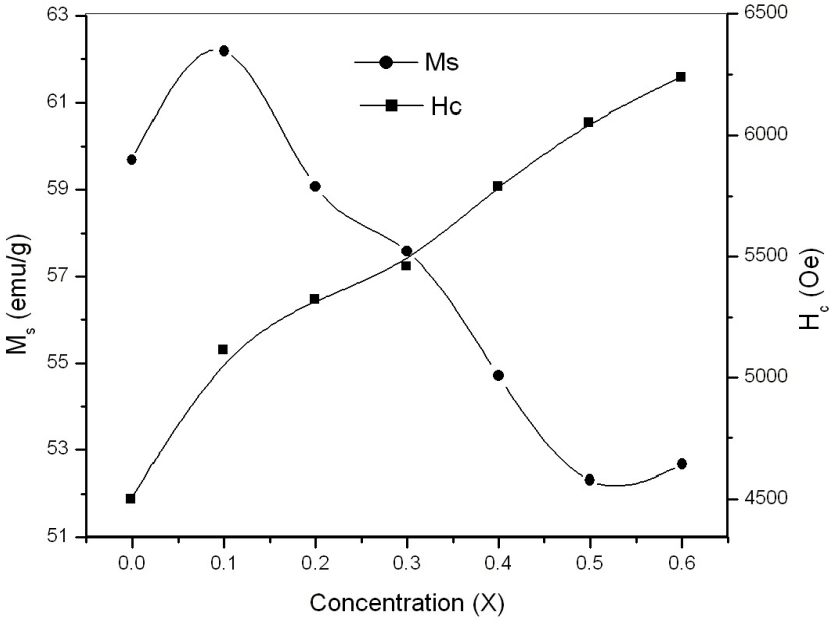

Fig. 3: Saturation magnetization and coercive fields versus Al concentration for strontium ferrite samples.

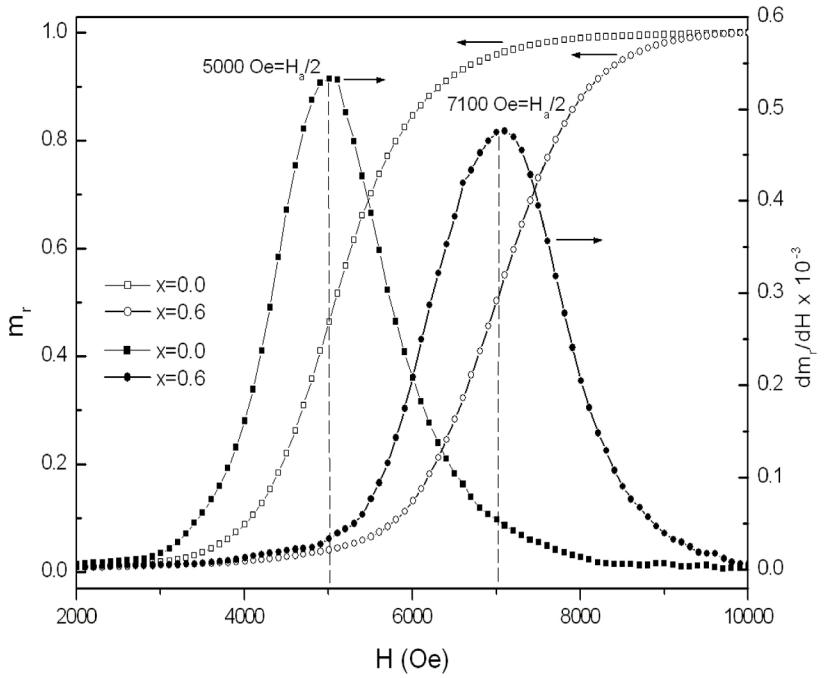

Fig. 4: Reduced isothermal remnant magnetization curves and corresponding SFD for the samples with x = 0.0 and x = 0.6.

have one Fe ion each, and 12*k* have six Fe ions. Figure 3 shows the saturation magnetization for $SrFe_{12-x}Al_xO_{19}$. For x=0.1 saturation magnetization increases from ~59.7 emu/g to 62.2 emu/g recording 4.2% increase in saturation magnetization. Which indicating that the substitution of Fe ions by non-magnetic Al ions occurs at spin-down sites ($4f_1$, $4f_2$). For x=0.5 the saturation magnetization decreases to ~52.3 emu/g recording 12.3% drop in saturation magnetization. This drop indicating that the replacement occurs at spin-up sites (2*a*, 2*b*, 12*k*).

Table 2 shows refined sites occupancies for all samples. The atomic number for Fe is 26 and for Al is 13. So site occupancy would be reduced if Fe ions replaced by Al one. According to the data in Table 2, we may conclude that for x=0.1 the replacement of Fe ions occurs most likely at $4f_1$ spin-down site. Since site occupancy changes from 0.0400 to 0.0387. For x=0.2 to x=0.5 the replacement occurs at 12*k* spin-up site. Since site occupancy changes from 0.12000 to 0.11583.

Table 2: Refined sites occupancy for $SrFe_{12-x}Al_xO_{19}$.

Atom	Site	Site Occupancy						
		x=0.0	x=0.1	x=0.2	x=0.3	x=0.4	x=0.5	X=0.6
Sr	2d	0.02000	0.02000	0.02000	0.02000	0.02000	0.02000	0.02000
Fe1	2a	0.02000	0.01996	0.01879	0.01875	0.01817	0.01828	0.01826
Fe2	2b	0.02000	0.01819	0.01878	0.01907	0.01876	0.01875	0.01875
Fe3	$4f_1$	0.04000	0.03868	0.03931	0.03972	0.03950	0.03906	0.03898
Fe4	$4f_2$	0.04000	0.04051	0.03982	0.04005	0.04081	0.03925	0.04001
Fe5	12k	0.12000	0.11767	0.11700	0.11650	0.11638	0.11583	0.11573
O1	4e	0.04000	0.04000	0.04000	0.04000	0.04000	0.04000	0.04000
O2	4f	0.04000	0.04000	0.04000	0.04000	0.04000	0.04000	0.04000
O3	6h	0.06000	0.06000	0.06000	0.06000	0.06000	0.06000	0.06000
O4	12k	0.12000	0.12000	0.12000	0.12000	0.12000	0.12000	0.12000
O5	12k	0.12000	0.12000	0.12000	0.12000	0.12000	0.12000	0.12000

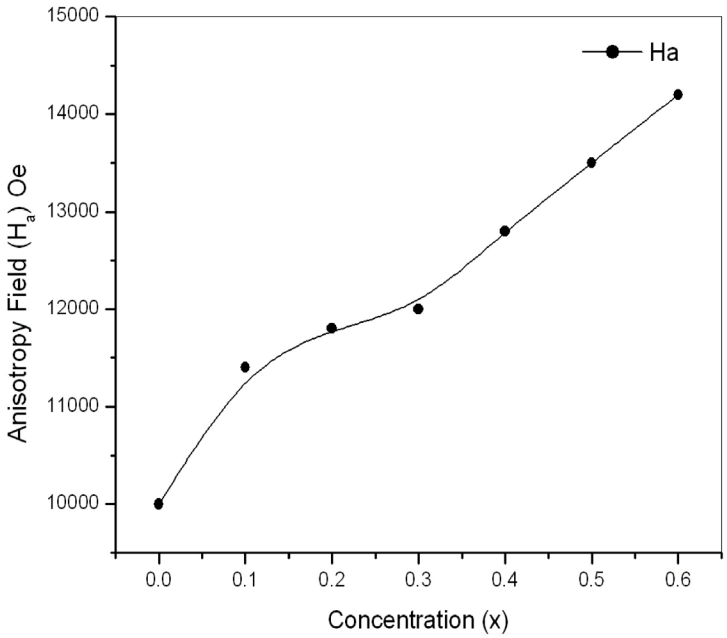

Fig. 5: Anisotropy field as a function of Al concentration of strontium ferrite samples.

Figure 3 also shows the coercive fields of $SrFe_{12-x}Al_xO_{19}$ as a function of *x*. As one might observe the value of the coercivity for pure sample is 4500 Oe, which agrees will with the literature value, since the coercivity of pure $SrFe_{12}O_{19}$ prepared by different methods was reported in the range (3500 – 5500) Oe [22, 23]. Also it is clear that doping of strontium ferrites with Al leads to significant increase in the coercivity as a result of the Al replacement of Fe^{3+}. The increase of the coercivity can be referred to the increase of the magnetic anisotropy field (H_a) as a result of Al substitution of Fe^{3+}.

We may enhance the above assumption by calculating the effective magnetic anisotropy field for the prepared samples from the maximum of switching field distribution (SFD) according to the equation[24]:

$$f\left(H\right)\Big]_{\max} = \left[dm_r/dH\right]_{H=H_a/2} \quad ...(3)$$

where $m_r(H) = M_r(H)/M_r(")$ is the reduced isothermal remnant magnetization (IRM), and dm_r/dH called switching field distribution (Figure 4). The magnetic anisotropy field (H_a) is equal to $2H_{max}$.

Figure 5 shows magnetic anisotropy field as a function of Al concentration. It is clear that H_a increase monotonically with increasing Al concentration up to x = 0.6, which might be the reason of enhancing the coercivity. It should be noted that, the increase in anisotropy field leads to increase in energy barriers, so the required field to reverse the magnetization become larger, which enhance the coercivity.

CONCLUSIONS

Strontium ferrite powders doped with different concentrations of aluminum ($SrFe_{12-x}Al_xO_{19}$) was prepared by solid state reaction method. Analyses of XRD measurements showed that all samples examined in this work of high quality. The replacement of Fe^{3+} with Al^{3+} ions in hexagonal strontium ferrite led to negligible changes in lattice constant *a*, whereas the hexagonal lattice constant *c* found to decrease with increasing the substitution amount of Al. Also it has been found that that Al^{3+} substitution for Fe^{3+} does not appreciably disturb the crystallinity of $SrFe_{12-x}Al_xO_{19}$, since the crystallite size for all samples ranged from 83 – 72 nm. The magnetic data showed that the doping of strontium with Al leads to a small decrease in saturation magnetization. While the coercivity increases as a result of increasing of the anisotropy field.

REFERENCES

1. El-Sayed S. M., Meaz T. M., Amer M. A., El Shersaby H. A., *Physica B*, **426***,* 137 (2013).
2. Marino-Castellanos P. A., Moreno-Borges A. C., Orozco-Melgar G., Garcia J. A., Govea-Alcaide E., *Physica B*, **406***,* 3130 (2011).
3. Slama J., Gruskova A., Papanova M., Kevicka D., Dosoudil R., Jancarik V., Gonzalez A., Mendoza G., *J. Magn. Magn. Mater,.* **272-276**, 385 (2004).
4. Awawdeh M., Bsoul I., H. Mahmood S., *J. Alloys Compd.*, **585**, 465 (2014).
5. Bsoul I., H. Mahmood S., *J. Alloys Compd.,* **489**, 110 (2010).
6. Sharma M., Kashyap S. C., Gupta H. C., *Physica B,* **448**, 24 (2014).
7. Herme C. A., Bercoff P. G., Jacobo S. E., *Physica B,* **407**, 3105 (2012).
8. Gonzalez-Angeles A., Mendoza-Suarez G., Gruskova A., Toth I., Jancarik V., Papanova M., Escalante-Garcia J. I., *J. Magn. Magn. Mater.*, **270**, 77 (2004).
9. Gonzalez-Angeles A., Mendoza-Suarez G., Gruskova A., Lipka J., Papanova M., Slama J., *J. Magn. Magn. Mater.,* **285***,* 450 (2005).
10. Gruskova A., Slama J., Dosoudil R., Kevicka D., Jancarik V., Toth I., *J. Magn. Magn. Mater,.* **242–245***,* 423 (2002).
11. Bsoul I., Mahmood S. H., Abdel-Fatah Lehlooh, Ahmed Al-Jamel, *J. Alloys Compd,.* **551***,* 490 (2013).
12. Bsoul I., Mahmood S. H., Abdel-Fatah Lehlooh, *J. Alloys Compd.*, **498**, 157 (2010).
13. Topal U., *Physica B,* **407**, 2058 (2012).
14. Topal U., Bakan H., *J. Eur. Ceram. Soc.*, **30**, 3167 (2010).
15. Topal U., *J. Alloys Compd,.* **320**, 331 (2008).
16. International Centre for Diffraction Data

(ICDD), File 00- 033-1340.
17. Obradors X., Solans X., Collomb A., Samaras D., Rodriguez J., Pernet M., Font-altaba M., *J. Solid State Chem,.* **72**, 218 (1988).
18. Warren B. E., *X-Ray Diffraction*, Addison-Wesley, Reading, Massachusetts, (1969).
19. An S. Y., Shim I. B., Kim C. S., *J. Appl. Phys.*, **91**, 8465 (2002).
20. Zhou X. Z., Morrish A. H., Li Z. W., Hong Y. K., *IEEE Trans. Magn.*, **27**,4654 (1991).
21. Williams J. M., Adetunji J., Gregori M., *J. Magn. Magn. Mater.,* **220**, 124 (2000).
22. Lu H.F., Hong R.Y., Li H.Z., *J. Alloys Compd.,* **509**, 10127 (2011).
23. Hessien M. M., Rashad M. M., El-Barawy K., *J. Magn. Magn. Mater.*, **320**, 336 (2008).
24. Pfeiffer H., Schüppel W., *Phys. Stat. Sol. (a)*, **119**, 259 (1990).